Constituent counting rule and ω photoproduction

Trevor Reed ⬤, Christopher Leon, Frank Vera, Lei Guo, and Brian Raue ⬤

Department of Physics, Florida International University, Miami, Florida 33199, USA

The constituent counting ruling (CCR) has been found to hold for numerous hard, exclusive processes. It predicts the differential cross section at high energies and fixed $\cos\theta_{\mathrm{c.m.}}$ should follow $\frac{d\sigma}{dt} \sim \frac{1}{s^{n-2}}$, where n is the minimal number of constituents involved in the reaction. Conversely, there are hard, exclusive processes for which it has been found that the CCR does not work. The exact reasons for these have not been clearly established. One such example, for which the analysis of CLAS data deviates from the prediction of the CCR, is the omega photoproduction reaction. Here, we provide an in-depth analysis of the reaction $\gamma p \to \omega p$ at $\theta_{\mathrm{c.m.}} \approx 90°$ using CLAS data with an energy range of $s = 5\text{--}8 \text{ GeV}^2$, where the CCR has been shown to work in other reactions. We argue for a stringent method to select data to test the CCR. Naïvely, this reaction would have $n = 9$ and we would expect a scaling of s^{-7}. Instead, a scaling of $s^{-(9.08\pm0.11)}$ was observed. A careful analysis of conservation of angular momentum is proposed to explain the discrepancy, supporting the validity of the CCR when applied properly.

DOI: 10.1103/PhysRevC.103.065203

I. INTRODUCTION

The transition from hadronic to partonic degrees of freedom is an interesting area of nuclear physics that is still not well understood. Knowing which kinematic regions have what effective degrees of freedom and how the transition between the two occurs can tell us much about quantum chromodynamics (QCD). Currently these problems are very difficult to solve purely through theoretical tools, and thus experiment can be used to provide guidance.

In the early days of QCD it was recognized that one of the consequences of having partons as the effective degree of freedom was the constituent counting rule (CCR) [1,2]. The rule states that for hard, exclusive processes the differential cross section should have the form

$$\frac{d\sigma}{dt} = \frac{f(\cos\theta_{\mathrm{c.m.}})}{s^{n-2}} = \frac{f(\cos\theta_{\mathrm{c.m.}})}{s^N}, \qquad (1)$$

where $\theta_{\mathrm{c.m.}}$ is the center-of-momentum scattering angle,[1] s and t are Mandelstam variables, N is the scaling parameter, and f is some function which, at least in principle, is calculable via QCD. Here $n = \sum_i n_i$ is the sum of the total number of constituents taking part in the hard subprocess. For elementary particles $n_e = 1$, for mesons $n_M = 2$, and for baryons $n_B = 3$. The rule is thought to be correct when the hardness of the

---

[1]From here on, any mention of the angle θ should be taken to be in the center-of-mass (c.m.) frame.

scattering is larger than the mass squared of any of the external particles $t \gtrsim \max_i(M_i^2)$ and at high energy $s \gg \max_i(M_i^2)$ (up to small corrections, such as logarithmic corrections due to renormalization).

The CCR can be justified on the basis of perturbative QCD (pQCD) and dimensional arguments. Specifically, in the QCD Feynman rules for scattering amplitudes the vertices have no dimension, gluon propagators have a dimensionality of inverse mass squared $\frac{1}{M^2}$, quark propagators have $\frac{1}{M}$, while external quarks have $\sqrt{M}$. Looking at a reaction with the minimal number of constituents where all participate, we need $\frac{n}{2} - 1$ virtual gluons, $\frac{n}{2} - 2$ virtual quarks, and n external quarks (see Fig. 1). It follows that the dimensionality of the scattering amplitude is $[\mathcal{M}] = \frac{1}{M^{2(\frac{n}{2}-1)}} \frac{1}{M^{\frac{n}{2}-2}} M^{n/2} = \frac{1}{M^{n-4}}$, which implies $[\frac{d\sigma}{dt}] = \frac{1}{M^{2(n-2)}}$ [3]. For a hard, exclusive QCD process there is only one mass scale, $\sqrt{s}$, and thus $\frac{d\sigma}{dt} \sim \frac{1}{s^{n-2}}$, with the dimensionless constant depending on the dimensionless degree of freedom, $\cos\theta$ (alternatively, $\frac{-t}{s}$). Additional gluon exchange and higher Fock state contributions are suppressed by additional factors of $\frac{1}{s}$. The above argument makes use of the approximate conformal symmetry of QCD, while a nonperturbative derivation has been made through the use of the AdS-CFT correspondence [4,5]. Including QED processes to describe meson photoproduction is straightforward.

The CCR has been found to hold for a number of reactions, often at surprisingly low energy and hardness scales. For example, in Ref. [6] it was shown that, for the reaction $\gamma p \to K^+\Lambda$, scaling of s^{-7} occurs for t values as low as 1.5 GeV^2 and s as low as 5 GeV^2 for $\cos\theta = 0$. Scaling at relatively low energy has also been observed with the photoproduction of pions. It was seen in Refs. [7,8] for $\gamma p \to \pi^+ n$
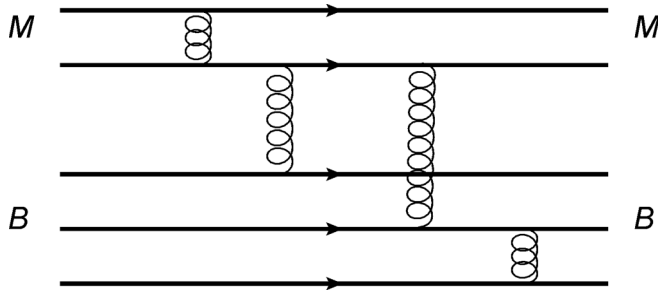
FIG. 1. Example of minimal diagram connecting all constituents for $MB \rightarrow MB$. Here there are $n = 10$ constituents or external quarks, $n/2 - 1 = 4$ gluon propagators, and $n/2 - 2 = 3$ quark propagators.

and $\gamma n \rightarrow \pi^- p$ for s approximately greater than 6.25 GeV^2 with $\theta = 90°$. The energy values (in terms of s) that are the focus of our work have a maximum value of 8.04 GeV^2 and go down to between approximately 5 and 6 GeV^2, depending on the angle (the cuts were made in terms of t). We will be looking at a kinematical range comparable to these previous studies.

In spite of the examples cited above, there has been mixed success of the CCR at intermediate energies and momentum transfers. A study of ten meson-baryon ($MB \rightarrow MB$) and baryon-baryon ($BB \rightarrow BB$) exclusive reactions at $\theta_{c.m.} = 90°$ and $-t \approx 5$ GeV^2 found that only three out of the ten reactions had $n - 2$ within 1σ of the expected result and only one other within 2σ [9]. Other apparent failures of the CCR led to the development of the handbag model and the use of generalized parton distributions (GPDs) in the study of deeply virtual Compton scattering [10–12] and hard meson production [13]. Arguments were made for the use of the handbag model in Compton scattering off the proton with moderate momentum transfer ($-t \leqslant 10$ GeV^2) [14]. A subsequent experiment at Jefferson Lab showed an extra suppression of $\frac{1}{s^2}$ for Compton scattering than the CCR predicted [15]. The results, however, were consistent with the handbag model.

Recently, there has been a discussion in the literature about the applicability, limitations, and necessary conditions for the CCR [16,17]. Reference [16] claims, "... were the constituent counting rule right, it would provide a very powerful and straightforward tool to access the valence quark structures of the exotic hadrons. But unfortunately ... for hadrons with hidden-flavor quarks it is problematic to apply such a naïve constituent counting rule." In contrast, Brodsky *et al.* [17] state "constituent counting rules are completely rigorous *when* they are applied properly." Given that the CCR has been suggested as a tool to study exotic hadrons, a good understanding of its correct application is needed. Here, we examine the issue by analyzing the data for a specific reaction.

A naïve application of the CCR to $\gamma p \rightarrow \omega p$ would suggest $n = n_\gamma + n_p + n_\omega + n_p = 1 + 3 + 2 + 3 = 9$, a scaling of $N = n - 2 = 7$, and thus $d\sigma/dt \sim s^{-7}$ for fixed $\cos \theta$. However, our analysis of the data is in fact more consistent with $d\sigma/dt \sim s^{-9}$. As discussed in Sec. IV, we provide a

theoretical argument that explains why the correct scaling power is $N = 9$.

II. DATA

The data being analyzed here were collected in the Jefferson Lab CLAS g11 experiment [18]. The relatively large number of events and low uncertainties of the $\gamma p \rightarrow \omega p$ reaction compared with other meson photoproduction data allowed for an in-depth analysis. The differential cross sections in the data set were converted via

$$\frac{d\sigma}{dt} = \frac{1}{2E_\gamma |\mathbf{p}_\omega|} \frac{d\sigma}{d\cos\theta_{c.m.}}, \quad (2)$$

where E_γ is the energy of the photon and $|\mathbf{p}_\omega|$ is the magnitude of the three-momentum of the ω meson in the c.m. frame.

The scaling of the cross section with the energy is ultimately a result of the point-like behavior of the scattering. Therefore, the CCR is expected to hold best when the $-t$ value is relatively large (hard scattering). Equally important for the unambiguous identification of a scaling trend is to avoid strong final-state interactions between the outgoing hadrons. Center-of-mass angles around $\theta = 90°$ are large enough that they reduce the chances of final-state interactions while not being so large that they introduce backscattering events, which include unwanted u-channel processes. Published experimental cross-section data frequently do not have bins corresponding exactly to $\cos \theta = 0$. Such is the case with the data set used in this analysis, and thus the four $\cos \theta$ bins -0.15, -0.05, $+0.05$, and $+0.15$ were examined. We will show in Sec. III that including several angle bins can be useful in getting the scaling parameter N at $\theta = 90°$. Most past analyses of the CCR use a cut in Mandelstam s (i.e., $s > s_0$), in conjunction with the large center-of-momentum angle criteria to select hard scattering events. We argue that $-t$ is the hardness of the scattering, so it should indicate the onset of pQCD. Other studies have correctly used hardness scales rather than energy to mark the onset of pQCD. For example, Ref. [19] used transverse momentum to determine scaling in the case of deuteron photodisintegration, which was found to work in the case of large angles. The specific use of $-t$ to define hardness was also employed in the case of polarized, wide-angle, Compton scattering [20]. Also, as can be seen in Fig. 2, a cut in s would still leave low $-t$ events, while a cut in $-t$ puts a lower limit on s. This can be seen easily in the massless limit where $-t = \frac{s}{2}(1 - \cos \theta)$. A lower limit for $-t$ imposes a lower limit for s since $(1 - \cos \theta) \leqslant 2$. However, for a given s, $-t$ can be made arbitrarily small when $\cos \theta \rightarrow 1$.

We selected data with $-t > 2$ GeV^2, resulting in 118 data points that met the criteria. The uncertainties considered were the statistical and point-to-point systematic uncertainties of the differential cross section $\frac{d\sigma}{d\cos\theta}$ included in the published data. The $-t$ cutoff value was chosen based on a natural energy scale considering the proton mass as well as observing a plateauing of the fit parameter N around $-t = 2$ GeV^2. In this region, the exact $-t$ cut selected has minimal impact on the results. This is demonstrated by Fig. 3. The range over $-t$ from about 1.5 to 2.5 GeV^2 has a relatively flat distribution of
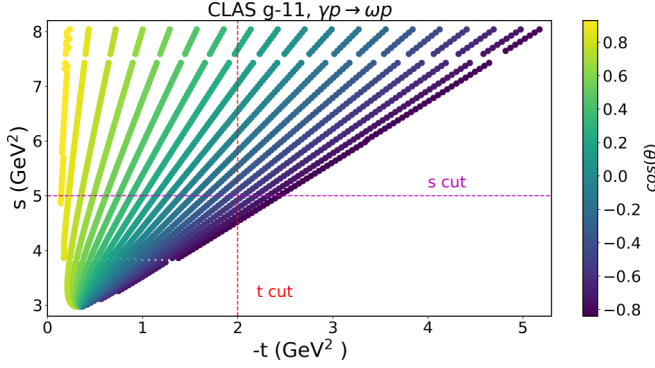
FIG. 2. Kinematics of the CLAS g11 ω photoproduction data. An s cut leaves low $-t$ events, but a $-t$ cut puts a lower bound on s.

the scaling parameter N. This plot also shows how poor the fits are in terms of the χ^2/df when the $-t$ cut is less than $1.5\,\text{GeV}^2$.

III. ANALYSIS

A. Scaling

In Fig. 4, the four angle bins around $\cos\theta = 0$ are shown with various scaling factors applied. Scaling of s^{-7} is clearly not observed for any of the angle bins. There appears to be some scaling like s^{-8} above $s = 6\,\text{GeV}^2$, but only for the $\cos\theta = -0.15$ bin. The scaling is most obvious in the s^{-9} case, where the distribution is quite flat for three of the four angles. Most importantly, the scaling is most extreme at the two $\cos\theta$ bins closest to zero: $\cos\theta = -0.05$ and $\cos\theta = +0.05$. This demonstrates that there is scaling as low as $s = 5\,\text{GeV}^2$, which agrees with observations for other reactions.
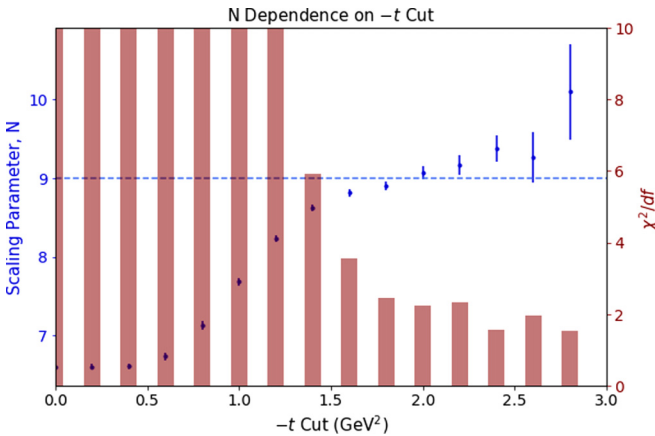

FIG. 3. The value returned for the fit parameter N as a function of the $-t$ cut is shown. The fitting function used is the Taylor series expansion form of the differential cross section from Eq. (3). The $-t$ value of each data point represents the minimum $|t|$ value allowed in the data set for that fit. The vertical bars show the reduced χ^2 for each fit. The reduced χ^2 values range from 83 to 13 over the $-t$ cut region of 0 to $1.4\,\text{GeV}^2$. The blue, horizontal, dashed line is added in at $N = 9$ to demonstrate the scaling of this value over a range of $-t$ cuts.
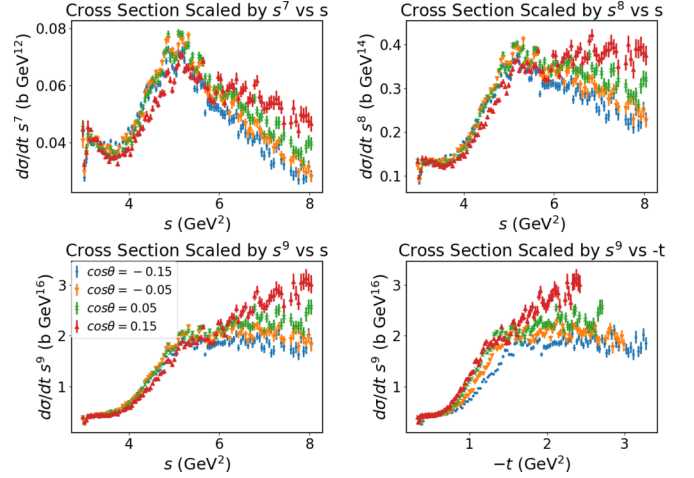

FIG. 4. The differential cross sections of the four angle bins nearest $\cos\theta = 0$ with three different scaling factors applied. s^9 scaling is shown for both s and $-t$ on the x axis.

The scaling is not what we would expect it to be based on simply adding up the constituents in the reaction. Scaling by s^9 (corresponding to $n = 11$) was found to work best, as can be seen in Fig. 4. For a given angle, the scaled $s^9 d\sigma/dt$ is nearly constant over the higher-s ranges, while without scaling, the cross section spans nearly two orders of magnitude.

B. Fits

The different angle bins can be fit with one function without explicit knowledge of $f(\cos\theta)$ by noting that, near $\cos\theta = 0$, a Taylor-series expansion can be taken: $f(\cos\theta) = A + B\cos\theta + O(\cos^2\theta)$. Keeping just the linear term, we can fit the function

$$\frac{d\sigma}{dt} = (A + B\cos\theta)s^{-N}. \quad (3)$$

Through this approach, data from multiple bins are used in the fit. Three different types of fits were performed on the data: χ^2 minimization, Bayesian estimation, and bootstrapping. No further details will be discussed for the χ^2 minimization method, given its ubiquitousness. However, the following will provide a brief explanation of how the two latter fitting techniques were done.

1. Bayesian estimation

In the Bayesian approach one conditions on the data $\mathcal{D}$. The posterior distribution for the parameters A, B, and N is proportional to the likelihood multiplied by the prior:

$$\mathcal{P}(A, B, N|\mathcal{D}) \propto \mathcal{P}(\mathcal{D}|A, B, N)\mathcal{P}(A, B, N). \quad (4)$$

Since N is the parameter of interest, one can then find the N posterior distribution $\mathcal{P}(N)$ by marginalizing out A, B. For the likelihood we take $\mathcal{P}(\mathcal{D}|A, B, N) = \exp(-\frac{1}{2}\chi^2)$.

First we assumed the three parameters to be independent, $\mathcal{P}(A, B, N) = \mathcal{P}(A)\mathcal{P}(B)\mathcal{P}(N)$. While not completely realistic, it is a starting point and with enough data a more accurate relation between the variables should emerge. Uniform distributions were used for all three variables, where for N we tried
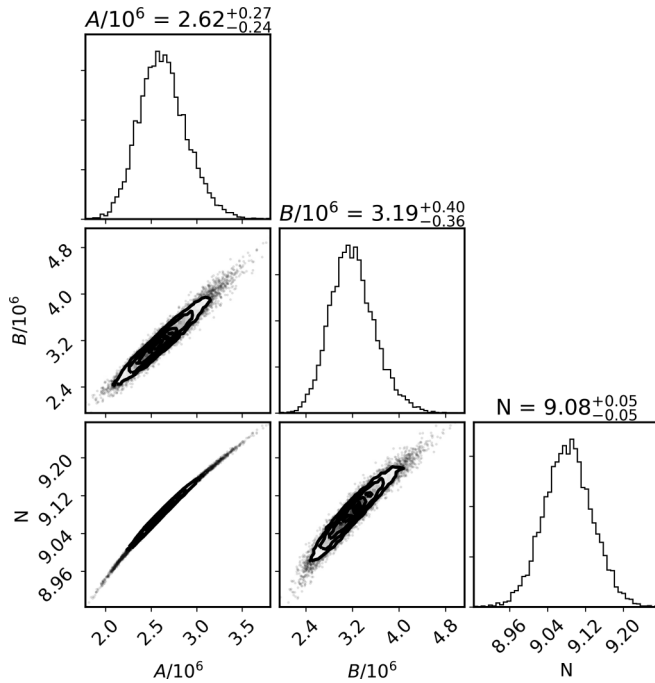
FIG. 5. Results of MCMC sampling. The graphs on the diagonal represent the histograms of each parameter and the off-diagonal graphs show the distributions in terms of each pair of parameters. Numbers above the parameter histograms indicate median and quintiles.

to capture our initial expectation that it should be around seven or eight but also allow some leeway by having it uniformly distributed between five and ten, $N \sim \mathcal{U}(5, 10)$. For A and B, we use $\mathcal{U}(10^4, 10^7)$. The likelihood function is the same as with the χ^2 approach. To get a representative sampling of parameter space we used a Markov chain Monte Carlo (MCMC) algorithm implemented through the library EMCEE [21]. The lower-right panel of Fig. 5 shows the marginalized posterior distribution for N and from the mean and standard deviation we get the Bayesian uniform prior estimate: $N_{BU} = 9.08 \pm 0.05$. Figure 6 shows the fit using the average values for the parameters.
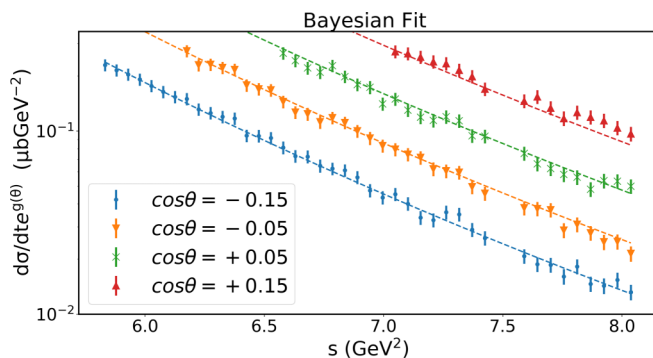

FIG. 6. The differential cross section fit with $(A + B \cos \theta)s^{-N}$, shown by the dash line. The data and fits were multiplied by $e^{g(\theta)}$ with $g(\theta) = 5(\cos \theta + 0.15)$ for readability.

TABLE I. Scaling parameter estimates.

Method	N	Comments
χ^2 minimization	9.07 ± 0.08	$\chi^2/df = 2.23$
Bayesian	9.08 ± 0.05	Uniform priors
Bootstrap	9.07 ± 0.06	Uniform distribution

To test the dependence on the prior we also tried a Gaussian distribution for N with the mean and standard deviation based on an earlier result [22], $N \sim \mathcal{N}(\mu = 7.2, \sigma^2 = 0.7^2)$. We obtained nearly identical results, suggesting that our results are not sensitive to the choice of priors.

2. Bootstrapping

The two methods above assume the likelihood is a Gaussian while in the Bayesian method we employed parametric distributions for the priors. As a check against these assumptions, we also made use of the nonparametric bootstrap method [23]. Each data point was resampled according to a uniform distribution centered at the value and a range of ± 2 times the uncertainty. The result was consistent with the two other fitting methods. Table I shows the results for the different methods.

C. Angle and cutoff dependence of scaling

Above, it was assumed that N is independent of $\cos \theta$. Renormalization arguments would suggest that N has some dependence on the transverse momentum transfer [24], thus on $\cos \theta$.[2]

To see the effects, we broadened the inclusion of angles to $-0.3 < \cos \theta < +0.3$ and for each bin took a fit of the form As^{-N}. Figure 7 shows how N depends on $\cos \theta$. The N value peaks near $\cos \theta = 0$, justifying our approximation that the scaling is independent from $\cos \theta$, although it is centered at $\cos \theta \approx -0.08$ rather than $\cos \theta = 0$. In the high-energy limit where everything is effectively massless, the transverse momentum of the reaction is $p_\perp^2 = \frac{tu}{s} = \frac{s}{4}(1 - \cos^2 \theta)$. Letting Λ_{QCD} be the QCD scale, then from renormalization and QCD one would then expect to see quantities to evolve in terms of

$$\ln \left(\frac{p_\perp^2}{\Lambda_{QCD}^2} \right) \simeq \ln \left(\frac{s}{4\Lambda_{QCD}^2} \right) + \cos^2 \theta + O(\cos^4 \theta), \quad (5)$$

which would explain the approximate $\cos^2 \theta$ dependence of N. Doing a quadratic fit for N in terms of $\cos \theta$ suggests $N(\cos \theta = 0) \approx 9.1$, consistent with our results and offering another way to estimate the scaling parameter at $\cos \theta = 0$ using multiple angle bins. Taking the four bins nearest $\cos \theta = 0$ we estimate the uncertainty due to the angle dependence to be $\delta N_\theta = (\sum_i \frac{1}{\delta N_i^2})^{-1/2} = 0.051$. A cutoff of

---

[2]A similar situation is expected in the large Bjorken x region for parton distribution functions (PDFs), where it is expected that the valence PDFs go like $f(x) \sim (1 - x)^N$ with $N = 3$ at low Q_0^2 but increase with Q^2 [25].
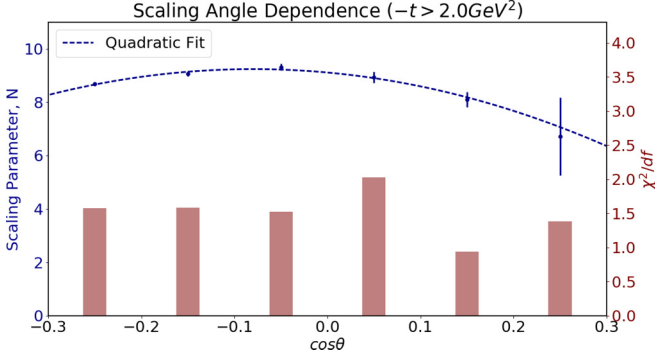
FIG. 7. Dependence on N with $\cos\theta$. Each bin was fit with the function As^{-N}.

$-t = 2.0\,\mathrm{GeV}^2$ was used. Table II summarizes the uncertainty results.

IV. DISCUSSION

The results obtained here contradict an earlier study that found $N = 7.2 \pm 0.7$ [22]. However, that result was based on only five data points and all of the points (except for one, which is from SLAC and has $s = 6.13\,\mathrm{GeV}^2$) have $s > 7\,\mathrm{GeV}^2$, going up to $s = 8.06\,\mathrm{GeV}^2$. Although these values are within the same range we are examining, they are not representative of the overall data set used in this analysis. The data discussed in this paper that pass the $-t > 2\,\mathrm{GeV}^2$ cut have s values that go down to as low as approximately $5.8\,\mathrm{GeV}^2$, depending on the angle. It is, however, fairly consistent with another analysis that found a scaling of $N = 9.4 \pm 0.1$ [26]. As mentioned before, a Compton-scattering experiment at Jefferson Lab also found an extra factor of $\frac{1}{s^2}$ from what was expected by CCR [15].

One possible explanation for the discrepancy between the naïve application of the CCR and the results of this analysis is that s and $-t$ are too low for it to be applicable. However, as mentioned earlier, the CCR does seem to explain other reactions at comparable energies and hardness scales. Also, this argument does not explain why it *does* work with $N = 9$.

We propose the following mechanism to explain the results: In Fig. 8, a model for ω photoproduction off the proton is presented. Since the reaction is at a high-enough energy, one can assume helicity conservation of quarks participating in the hard scattering subprocess. The matrix elements with vertices $\gamma_{\mu_i}^T$ ($i = 1, 2, 3$) are constrained to be transverse because they coupled to vector bosons (photon and meson) with transverse polarization states.

TABLE II. Fit systematic uncertainties.

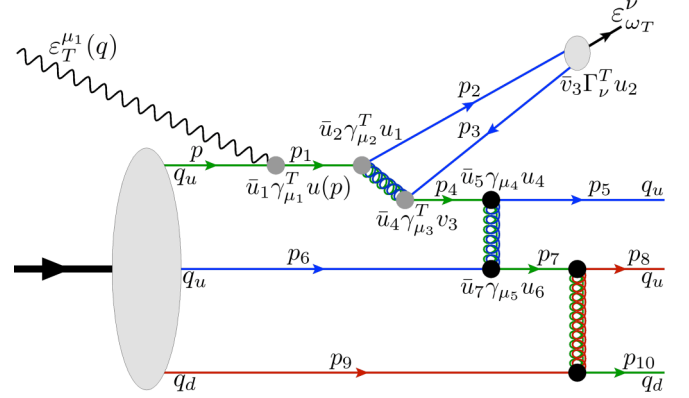| Source of uncertainty	δN Estimate
Fit	0.051
Angle dependence	0.067
$-t$ cutoff dependence	0.072

FIG. 8. Diagram for ω photoproduction. The polarization vectors of the photon $\varepsilon_T^{\mu_1}$ and vector meson $\varepsilon_{\omega_T}^{\nu}$ are constrained to be transverse.

Consider the photon-quark interaction $\gamma_{\mu_1}^T$ in the Breit frame of the quark represented by the spinor of $u(p)$. In this frame, the quark has no transverse momentum ($p_\perp = 0$), thus there is no orbital angular momentum to account for. Since in the Breit frame the momentum flips, $\vec{p} = -\vec{p}_1$, helicity conservation implies that the spin must also flip. Using Tables II and III from Appendix A of Ref. [27], we can see there is a suppression of one power of s at each of the vertices γ_{μ_1} and γ_{μ_2}. For $\gamma_{\mu_3}^T$, there is no suppression if we demand $p_2^T \sim p_3^T \sim p_2^+ \sim p_3^+$, i.e., $t \sim s$, which happens at large angles. If $t \sim s$ is not fulfilled there is an extra power suppression at $\gamma_{\mu_3}^T$ as well. Overall, the power counting is of two powers of s more than the naive one, leading to $N = 11 - 2 = 9$. Thus, a careful consideration of conservation of angular momentum to the CCR explains why $d\sigma/dt$ in the photoproduction of the spin$-1\,\omega$ behaves differently from that of scalar mesons. Given that the ρ^0 meson is also spin-1 and has a similar quark structure to the ω, we predict a similar scaling should follow.

V. CONCLUSION

In this analysis, we have examined the published CLAS g11 data for s scaling in ω photoproduction. We demonstrated and argued the advantage of cutting by the relevant hardness parameter $-t$ (rather than s) and combining several angle bins through a Taylor expansion of the $\cos\theta$-dependent function of $\frac{d\sigma}{dt}$. Around $\theta = 90°$, we found the scaling to be $N = 9.08 \pm 0.11$, inconsistent with a naïve application of the CCR. We have made the case for additional gluon exchanges and spin-flipping to conserve helicity. Further exploration of these mechanisms are warranted. Future CLAS12, GlueX, and the CLAS g12 experiment (E_γ up to 5.45 GeV) data for this reaction at higher energy scales could be used to examine if this trend continues into higher energies. Other reactions from these experiments could also be tested against our observations. Our results suggest that the CCR is in fact valid for the examined data. However, the data selection must be based on

hardness of the scattering, using $-t$ instead of s. It is thus worth pointing out that, when applied appropriately, the CCR could also be used to investigate exotic hadrons such as hybrid mesons to be studied in the GlueX experiment [28], where a range of beam energies will make an analysis similar to ours possible.

[1] S. J. Brodsky and G. R. Farrar, Phys. Rev. Lett. **31**, 1153 (1973).

[2] S. J. Brodsky and G. R. Farrar, Phys. Rev. D **11**, 1309 (1975).

[3] H. Kawamura, S. Kumano, and T. Sekihara, Phys. Rev. D **88**, 034010 (2013).

[4] J. Polchinski and M. J. Strassler, Phys. Rev. Lett. **88**, 031601 (2002).

[5] S. J. Brodsky and G. F. de Téramond, Subnuclear Series **45**, 139 (2009).

[6] R. A. Schumacher and M. M. Sargsian, Phys. Rev. C **83**, 025207 (2011).

[7] H. Gao, Mod. Phys. Lett. A **18**, 215 (2003).

[8] L. Y. Zhu *et al.*, Phys. Rev. C **71**, 044603 (2005).

[9] C. White *et al.*, Phys. Rev. D **49**, 58 (1994).

[10] A. V. Radyushkin, Phys. Lett. B **380**, 417 (1996).

[11] X. Ji, Phys. Rev. Lett. **78**, 610 (1997).

[12] X. Ji, Phys. Rev. D **55**, 7114 (1997).

[13] A. V. Radyushkin, Phys. Lett. B **385**, 333 (1996).

[14] A. V. Radyushkin, Phys. Rev. D **58**, 114008 (1998).

[15] A. Danagoulian *et al.*, Phys. Rev. Lett. **98**, 152001 (2007).

[16] F.-K. Guo, U.-G. Meißner, and W. Wang, Chin. Phys. C **41**, 053108 (2017).

[17] S. J. Brodsky, R. F. Lebed, and V. E. Lyubovitskij, Phys. Rev. D **97**, 034009 (2018).

[18] M. Williams *et al.*, Phys. Rev. C **80**, 065208 (2009).

[19] C. Bochna *et al.*, Phys. Rev. Lett. **81**, 4576 (1998).

[20] C. Fanelli *et al.*, Phys. Rev. Lett. **115**, 152001 (2015).

[21] D. Foreman-Mackey, D. W. Hogg, D. Lang, and J. Goodman, Publ. Astron. Soc. Pac. **125**, 306 (2013).

[22] M. Battaglieri *et al.*, Phys. Rev. Lett. **90**, 022002 (2003).

[23] B. Efron, Ann. Stat. **7**, 1 (1979).

[24] D. Sivers, S. J. Brodsky, and R. Blankenbecler, Phys. Rep. **23**, 1 (1976).

[25] R. J. Holt and C. D. Roberts, Rev. Mod. Phys. **82**, 2991 (2010).

[26] B. Dey, Phys. Rev. D **90**, 014013 (2014).

[27] G. P. Lepage and S. J. Brodsky, Phys. Rev. D **22**, 2157 (1980).

[28] S. Adhikari *et al.* (GlueX Collaboration), Nucl. Instrum. Meth. A **987**, 164807 (2021).